lumen covered by endothelial cells and was scored from 1 to 3 (1=25%; 2=25% to 75%; 3=>75%).

The distal part of the stent was used for either fluorescence or pathological analysis after the stent struts were gently removed with micro-forceps. For fluorescence microscopic analysis, the tissue was frozen and subjected to cryosection (5-μm) and counterstain with propidium iodide and examined using fluorescence microscopy. At least 5 high-power field pictures from 2 to 3 sections were taken, and cells positive with nuclear or peri-nuclear FITC among cells with nuclear propidium iodide positivity.

References

1. Okada H, Inoue Y, Heya T, Ueno H, Ogawa Y, Toguchi H. Pharmacokinetics of once-a-month injectable microspheres of leuprolide acetate. *Pharm Res.* 1991;8:787-91.
2. Ohtani K, Egashira K, Nakano K, Zhao G, Funakoshi K, Ihara Y, Kimura S, Tominaga R, Morishita R, Sunagawa K. Stent-based local delivery of nuclear factor-kappaB decoy attenuates in-stent restenosis in hypercholesterolemic rabbits. *Circulation.* 2006;114:2773-9.
3. Ohtani K, Usui M, Nakano K, Kohjimoto Y, Kitajima S, Hirouchi Y, Li XH, Kitamoto S, Takeshita A, Egashira K. Antimonocyte chemoattractant protein-1 gene therapy reduces experimental in-stent restenosis in hypercholesterolemic rabbits and monkeys. *Gene Ther.* 2004;11:1273-82.
4. Suzuki T, Kopia G, Hayashi S, Bailey LR, Llanos G, Wilensky R, Klugherz BD, Papandreou G, Narayan P, Leon MB, Yeung AC, Tio F, Tsao PS, Falotico R,

Carter AJ. Stent-based delivery of sirolimus reduces neointimal formation in a porcine coronary model. *Circulation*. 2001;104:1188-93.

Supplementary Table. Re-Endothelialization, Injury Score, and Inflammation Score 4 Weeks After Stenting

	Bare metal control stent (n= 8)	NP-eluting stent (n= 8)	Polymer-coated stent (n=3)	P value
Re-endothelialization (%)	3 ± 0	3 ± 0	3 ± 0	*1.0*
Injury score	1.77 ± 0.08	1.81 ± 0.08	1.77 ± 0.08	*0.84*
Inflammation score	1.60 ± 0.14	1.63 ± 0.07	1.42 ± 0.26	*0.58*

Data are Mean ± SE.

The degrees of endothelial recovery in the three groups are also shown. The endothelialization score was defined as the extent of the circumference of the arterial lumen covered by endothelial cells and was scored from 1 to 3 (1=25%; 2=25% to 75%; 3=>75%).

The injury score was determined at each strut site, and mean values were calculated for each stented segment. In brief, a numeric value from 0 (no injury) to 3 (most injury) was assigned: 0 = endothelial denudate, internal elastica lamina (IEL) intact; 1 = IEL lacerated, media compressed, not lacerated; 2 = IEL lacerated, media lacerated, external elastica lamina (EEL) compressed, not lacerated; and 3 = media severely lacerated, EEL lacerated, adventitial may contain stent strut. The average injury score for each segment was calculated by dividing the sum of injury scores by the total number of struts at the examined section.

The inflammation score took into consideration the extent and density of the inflammatory infiltrate in each individual strut. With regard to the inflammatory score for each individual strut, the grading is: 0 = no inflammatory cells surrounding the strut; 1 = light, noncircumferential inflammatory cells infiltrate surrounding the strut; 2 = localized, moderate to dense cellular aggregate surrounding the strut noncircumferentially; and 3 = circumferential dense inflammatory cells infiltration of the strut. The inflammatory score for each cross section was calculated in the same manner as for the injury score (sum of the individual inflammatory scores, divided by the number of struts in the examined section).

Reference

Schwartz RS, Huber KC, Murphy JG, Edwards WD, Camrud AR, Vlietstra RE, Holmes DR. Restenosis and the proportional neointimal response to coronary artery injury: results in a porcine model. *J Am Coll Cardiol.* 1992;19:267-74.

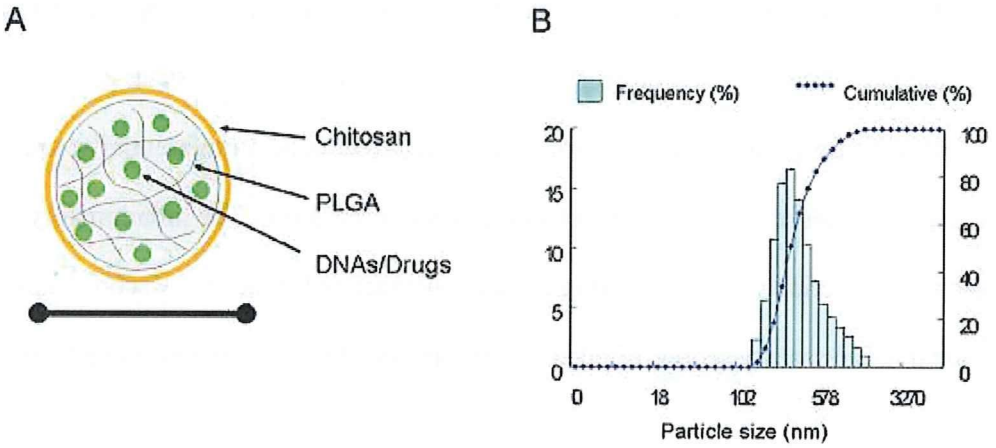

Supplementary Figure I. Schematic illustration of NP and NP size distribution. (A) Preparation of cationic PLGA NP with surface modification with chitosan. We prepared bioabsorbable poly-lactide-glycolide copolymer (PLGA) nanoparticle (NP) by emulsion solvent diffusion method. This NP system included followed advantages.

1. The matrix polymer (PLGA) is bioabsorbable and safe.
2. NP can incorporate water-soluble drugs/oligonuleotides/DNAs.
3. NP can cross cell membrane via endocytosis (efficiency of cellular uptake: 90 % or more), and deliver the encapsulated agents into the cytoplasm.
4. Incorporated drugs are slowly released from NP with hydrolysis of PLGA, which works intracellular DDS after intracellular uptake.
5. Surface change can be controlled at cationic state by addition of chitosan on surface.

(B) Particle size distribution of FITC-incorporated PLGA nanoparticles in water.

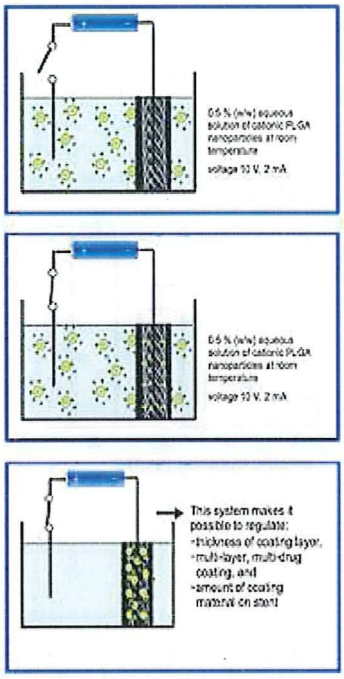

Supplementary Figure II. Schematic illustration of the electrodeposition coating system (chamber, electrodes, and DC power supply) for a cation nanoparticle coating technology. Three steps of electrodeposit coating procedure are shown.

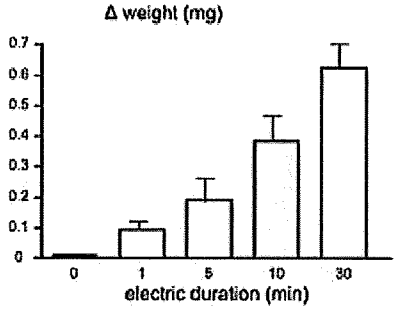

Supplementary Figure III. Amount of coating of NP (Δ stent weight) on the surface of stents increased with period of electricity (n=4 each). Weight of stent was measured before and after cationic electrodeposit coating of NP on stents. Data are mean ± SEM.

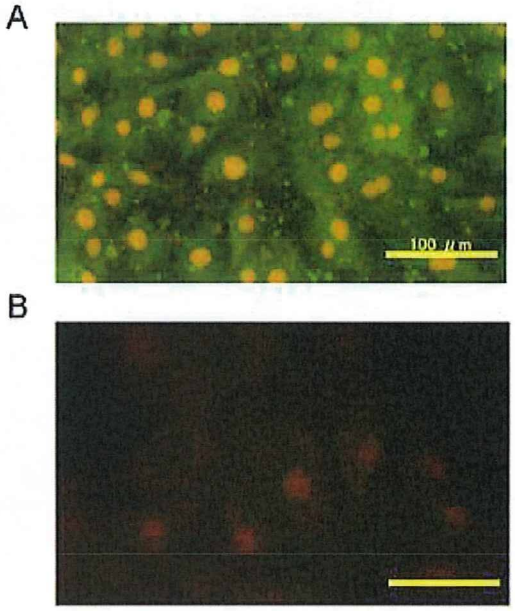

Supplementary Figure IV. Fluorescence microscopic pictures of human coronary artery smooth muscle cells 1 hour after the addition of NP eluted from FITC-NP-eluting stent (A) and 1 hour after addition of FITC-PLGA matrix eluted from PLGA polymer-based FITC-eluting stent (B). Cellular positivity was 99-100 % (n= 6) and 10 % or less in A and B, respectively. Bar = 100 μm.

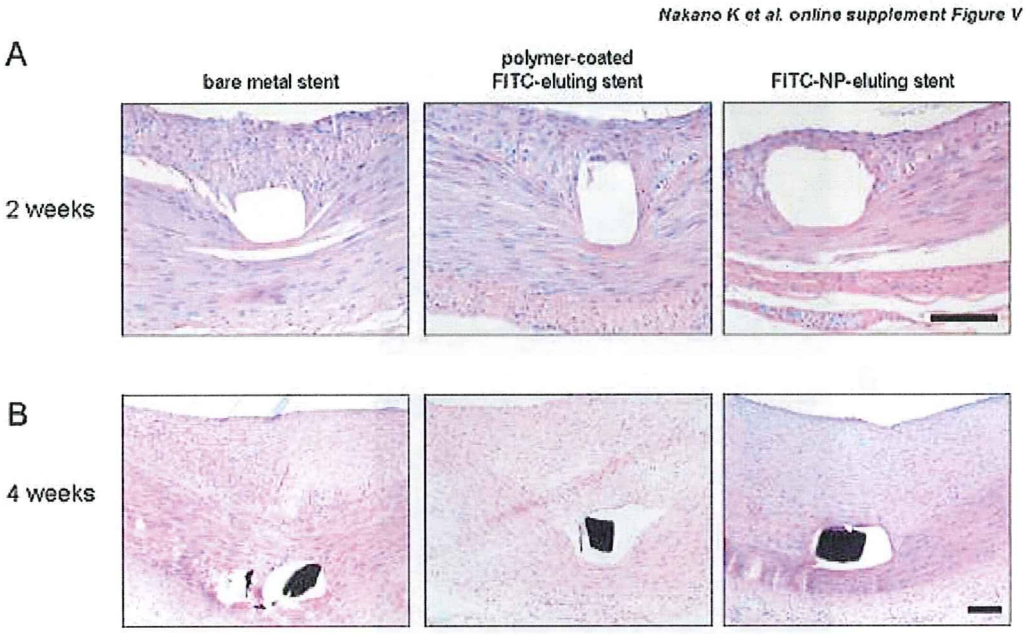

Supplementary Figure V. Micrographs of cross section stained with Hematoxylin-Eosin from coronary artery treated with bare metal stent, polymer-coated FITC-eluting stent and FITC-NP-eluting stents.

A, High-power photomicrographs around stent strut 2 weeks after stenting in porcine coronary arteries. Bar = 100 μm.

B, High-power photomicrographs around stent strut weeks after stenting in porcine coronary arteries. Bar = 100 μm.

Therapeutic Neovascularization by Nanotechnology-Mediated Cell-Selective Delivery of Pitavastatin Into the Vascular Endothelium

Mitsuki Kubo, Kensuke Egashira, Takahiro Inoue, Jun-ichiro Koga, Shinichiro Oda, Ling Chen, Kaku Nakano, Tetsuya Matoba, Yoshiaki Kawashima, Kaori Hara, Hiroyuki Tsujimoto, Katsuo Sueishi, Ryuji Tominaga, Kenji Sunagawa

Objective—Recent clinical studies of therapeutic neovascularization using angiogenic growth factors demonstrated smaller therapeutic effects than those reported in animal experiments. We hypothesized that nanoparticle (NP)-mediated cell-selective delivery of statins to vascular endothelium would more effectively and integratively induce therapeutic neovascularization.

Methods and Results—In a murine hindlimb ischemia model, intramuscular injection of biodegradable polymeric NP resulted in cell-selective delivery of NP into the capillary and arteriolar endothelium of ischemic muscles for up to 2 weeks postinjection. NP-mediated statin delivery significantly enhanced recovery of blood perfusion to the ischemic limb, increased angiogenesis and arteriogenesis, and promoted expression of the protein kinase Akt, endothelial nitric oxide synthase (eNOS), and angiogenic growth factors. These effects were blocked in mice administered a nitric oxide synthase inhibitor, or in eNOS-deficient mice.

Conclusions—NP-mediated cell-selective statin delivery may be a more effective and integrative strategy for therapeutic neovascularization in patients with severe organ ischemia. (***Arterioscler Thromb Vasc Biol.* 2009;29:796-801.)**

Key Words: nanotechnology ■ drug delivery system ■ statin ■ therapeutic neovascularization

Restoration of tissue perfusion in patients with critical ischemia attributable to coronary artery disease and peripheral artery disease is a major therapeutic goal. Recently, double-blind placebo-controlled clinical trials designed to induce neovascularization by administering exogenous angiogenic growth factors failed to demonstrate a clinical benefit and produced some undesired side effects.[1,2] These nonoptimal clinical results were in contrast to the results obtained in animal experiments and small open-label clinical trials.[3,4] The disappointing results of the clinical trials of therapeutic angiogenesis may be attributable in part to less effective transfection of the genetic materials or the rapid washout of proteins. In addition, because the involvement of multiple endogenous angiogenic growth factors is required for the development of functional collaterals,[5,6] the strategy of simple intramuscular injection of an exogenous angiogenic growth factor is limited. A high local concentration of angiogenic growth factors increases the risks of edema,[3,7] angioma-like capillary formation,[7–9] atherosclerosis after vascular injury,[10–13] and tumor-angiogenesis.[7,8] A controlled drug delivery system (DDS) for an integrative approach to therapeutic neovascularization would be more favorable.

To address this challenge, we developed a novel nanoparticle (NP)-mediated DDS, formulated from the bioabsorbable polylactide/glycolide copolymer (PLGA).[14] The PLGA NP offers the advantages of safety, delivery of encapsulated drugs into the cellular cytoplasm, and slow cytoplasmic drug release.[14,15] PLGA NP are effectively and rapidly taken up by vascular endothelial cells in vitro.[16] To our knowledge, however, no prior studies have examined whether PLGA NPs are useful as an endothelial cell-selective DDS in vivo.

We hypothesized that HMG-CoA reductase inhibitors, so-called statins, are appropriate candidate drugs for this integrative approach, because statins have a variety of pleiotropic vasculoprotective effects that are independent of their lipid-lowering activity.[17] Statins increase the angiogenic activity of mature endothelial cells as well as that of endothelial progenitor cells (EPCs)[18,19] and augment collateral growth in ischemic heart and limb in experimental animals.[20,21] In addition, statins attenuate atherosclerosis formation[22,23] and have little potential risk of tumor angiogenesis in contrast to angiogenic growth factors.[24] Most of these beneficial effects of statin on therapeutic neovascularization, however, were observed after daily administration of high doses,[18–21] which

Received December 9, 2008; revision accepted March 16, 2009.

From the Department of Cardiovascular Medicine (M.K., K.E., T.I., J.K., L.C., K.N., T.K., K. Sunagawa), Surgery (S.O., R.T.), and Pathology (K. Sueishi), Graduate School of Medical Sciences, Kyushu University, Fukuoka, Japan; the School of Pharmaceutical Science (Y.K.), Aichi Gakuin University, Aichi, Japan; and Hosokawa Powder Technology Research Institute (K.H., H.T.), Osaka, Japan.

Correspondence to Kensuke Egashira, MD, PhD, Department of Cardiovascular Medicine, Graduate School of Medical Science, Kyushu University, 3-1-1, Maidashi, Higashi-ku, Fukuoka 812-8582, Japan. E-mail egashira@cardiol.med.kyushu-u.ac.jp

Arterioscler Thromb Vasc Biol **is available at http://atvb.ahajournals.org** **DOI: 10.1161/ATVBAHA.108.182584**

may lead to serious adverse side effects in a clinical setting. Because vascular endothelium plays a primary role in the pathogenesis of ischemia-induced neovascularization, we hypothesized that NP-mediated cell-selective delivery of statins to the vascular endothelium would more effectively and integratively induce therapeutic neovascularization.

The major aim of this study was to test the hypothesis that selective NP-mediated delivery of statins to endothelial cells can be an integrative approach to enhance therapeutic neovascularization. We used a murine model of hindlimb ischemia to examine, (1) whether PLGA NPs are delivered selectively to vascular endothelial cells in ischemic tissues; and (2) whether NP-mediated delivery of statin is useful for increasing therapeutic neovascularization.

Materials and Methods

Preparation of PLGA NPs

Anionic PLGA NPs encapsulated with fluorescein isothiocyanate (FITC) or pitavastatin were prepared by a previously reported emulsion solvent diffusion method in purified water. The diameter of the PLGA NPs was 196±29 nm. The PLGA NPs had a negative surface charge (-15±10 mV). The FITC- and pitavastatin-loaded PLGA NPs contained 5% (wt/vol) FITC and 5% (wt/vol) pitavastatin, respectively. Additional details are provided in the supplemental information (please see http://atvb.ahajournals.org.).

Intracellular Uptake and Intracellular Distribution of NPs

Human umbilical vein endothelial cells (HUVECs) were obtained and cultured in EGM-2. Human skeletal muscle cells (SkMCs) were obtained and cultured in SkGM. Additional details can be found in the supplemental information.

Angiogenesis Assay of Human Endothelial Cells

Angiogenesis assay of human endothelial cells was tested using a 2-dimensional Matrigel assay. Additional details are provided in the supplemental information.

Animal Preparation and Experimental Protocol

Male 8-week-old C57BL/6J wild-type mice were used. After anesthesia, we induced unilateral hindlimb ischemia in the mice as previously described.[25] Immediately after the induction of ischemia, animals were randomly divided into 4 groups; a control no treatment group and the remaining groups received intramuscular injections of FITC-NPs (NP group), pitavastatin at 0.4 mg/kg (statin only group), or pitavastatin-NPs containing 0.4 mg/kg pitavastatin (statin-NP group) into the left femoral and thigh muscles. Biochemical parameters listed in supplemental Table I were measured 3, 7, and 14 days after treatment. Additional details are provided in the supplemental information.

Limb blood flow measurements were performed using a laser Doppler perfusion imaging (LDPI) analyzer (Moor Instruments). The LDPI index was expressed as the ratio of the LDPI signal in the ischemic limb compared to that in the normal limb.[25]

Histological and Immunohistochemical Analyses

Histological and immunohistochemical evaluation was performed. To determine capillary and arteriolar density, cross sections were stained with anti-mouse platelet endothelial cell adhesion molecule (PECAM)-1 antibody (CD31) and α-smooth muscle actin (α-SMA), respectively. Additional details are provided in the supplemental information.

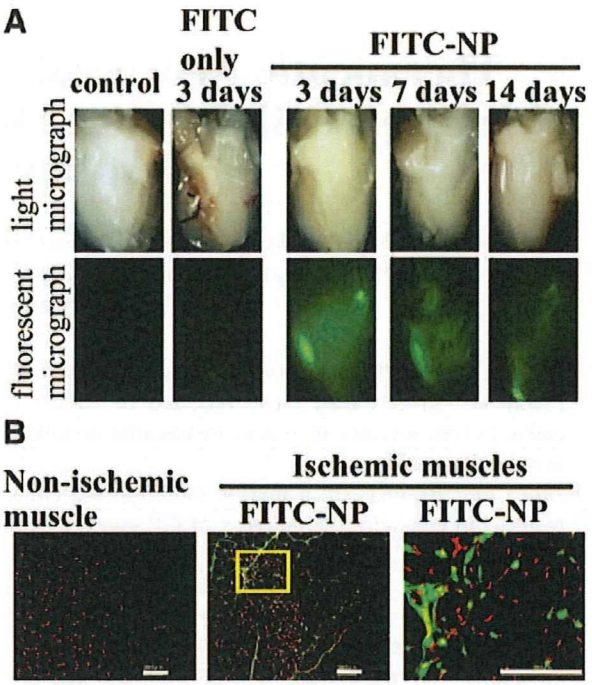

Figure 1. A, Representative light and fluorescent stereomicrographs of gastrocnemius muscles from control nonischemic hindlimb and from ischemic hindlimb. B, Fluorescent micrographs of cross-sections from nonischemic muscle with no injection, ischemic muscles 14 days after the injection of FITC-NP, and expanded view of boxed area of middle panel. Scale bars: 100 μm.

Western Blotting

Protein expression of Akt, eNOS, VEGF, FGF-2, and MCP-1 was examined 7 days after the induction of hindlimb ischemia. Additional details are provided in the supplemental information.

Flow Cytometric Analyses of EPC Mobilization

Peripheral blood was obtained from mice 7 and 14 days after hindlimb ischemia and analyzed with a FACS Caliber flow cytometer (Becton Dickinson). Additional details are provided in the supplemental Information.

Measurements of Statin Concentration in Serum and Muscle Tissue

Statin concentration in serum and muscle were measured at predetermined time points using a column-switching high performance liquid chromatography system. Additional details are provided in the supplemental information.

Statistical Analysis

Data are expressed as means±SEM. The statistical analysis was assessed using analysis of variance and multiple comparison tests. Probability values less than 0.05 were considered to be statistically significant.

Results

Cell-Selective Delivery of NPs In Vivo

Cellular distribution of FITC was examined 3, 7, and 14 days after intramuscular injection of FITC-NP or FITC only. On day 3 postinjection, strong FITC signals were detected only in FITC-NP injected ischemic muscle, whereas no FITC signals were observed in control nonischemic muscle or in ischemic muscle injected with FITC only (Figure 1A). The FITC

signals were localized predominantly in the capillaries and arterioles. FITC signals were also detected in myocytes at this time point. These data suggest that NP solution might distribute to intra- and extracellular spaces of ischemic skeletal muscle tissues immediately after intramuscular injection of NPs, and then the NP was uptaken by cells in injected muscles (endothelial cells, smooth muscle cells, myocytes, etc) or retained in extracellular spaces at this early time point.

On days 7 and 14, FITC signals remained localized predominantly in capillaries and arterioles (Figure 1B). Immunofluorescent staining revealed FITC signals localized mainly in endothelial cells positive for CD31, a marker of angiogenesis, in FITC-NPs injected ischemic muscle 14 days postischemia (supplemental Figure I). In contrast, no FITC signals were observed in myocytes. FITC signals were not detected in contralateral nonischemic hindlimb or in remote organs (liver, spleen, kidney, and heart) at any time point (data not shown).

Cellular Delivery of NPs Into Vascular Endothelial Cells Versus Skeletal Myocytes In Vitro

Cellular uptake of NPs was examined in HUVECs and SkMCs after incubation with FITC-NPs for 1 hour. The number of FITC-positive cells was greater among HUVECs than among SkMCs (supplemental Figure IIA). An inhibitor of clathrin-mediated endocytosis, chlorpromazine (CPZ), did not affect the magnitude of cellular FITC signals in SkMCs, but reduced the magnitude in HUVECs (supplemental Figure IIB). Long-term cell culture after 1-hour incubation with FITC-NPs revealed cellular FITC signals in HUVECs on days 3 and 7 postincubation (supplemental Figure IIC). In contrast, no FITC signal was detected in SkMC (data not shown).

Effects of Statin-NP on Ischemia-Induced Neovascularization

Treatment with statin-NP that contains pitavastatin at 0.4 mg/kg, but not with FITC-NP or statin only, significantly increased blood flow recovery on days 7 and 14 (Figure 2A and 2B). The beneficial effects of statin-NP were not associated with significant changes in serum biochemical markers (supplemental Table I), but angiogenesis and arteriogenesis were significantly increased (Figure 2C). Examination of hematoxylin-eosin-stained sections revealed no abnormal histopathologic findings (inflammation and fibrosis) among the 4 groups (data not shown). There was no significant difference in muscle fiber density among the 4 groups (data not shown).

Single intramuscular injection of nonnanoparticulated soluble pitavastatin at doses of 4 and 20 mg/kg exerted no effect on blood perfusion after hindlimb ischemia (supplemental Figure IIIA). Oral daily administration of pitavastatin at 0.4 mg/kg did not increase blood flow recovery, but pitavastatin at 1.0 and 10 mg/kg significantly increased blood flow recovery on day 14 (supplemental Figure IV).

Systemic daily administration of statins is reported to increase EPC mobilization,[18,26] but the EPC number in the circulating blood was not increased in the present study (supplemental Figure IIIB and IIIC). No therapeutic effects of

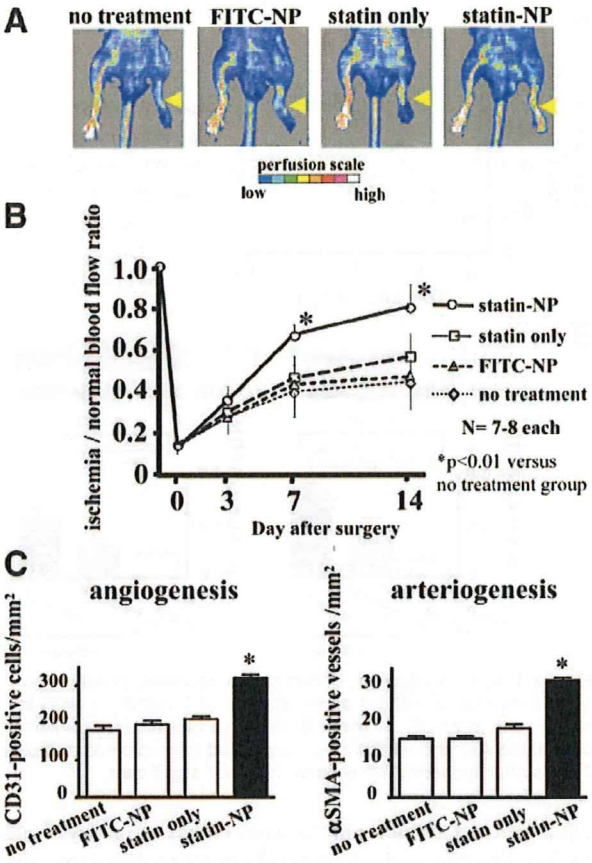

Figure 2. A, Representative laser Doppler perfusion imaging at 14 days postischemia. Arrow indicates ischemic limb. B, Quantification of blood flow recovery. C, Quantitative analysis of angiogenesis and arteriogenesis. n=4 each. *$P<0.01$ vs no treatment group.

statin-NP were observed in wild-type mice administered L-NAME or in eNOS$^{-/-}$ mice (Figure 3A), suggesting that eNOS-related signals are involved in the mechanism of statin-induced enhancement of ischemia-induced neovascularization (supplemental Figure V). Treatment with statin-NP increased both phosphorylated eNOS and serine-threonine specific protein kinase (Akt) in ischemic muscles compared with nonischemic control and nontreated ischemic muscles at 7 days of treatment (Figure 3B). Immunohistochemistry revealed that the increased eNOS and Akt activities were localized mainly in microvascular endothelial cells (supplemental Figure VI).

Effect of Statin-NP on Endogenous Angiogenic Growth Factor Expression

Immunohistochemistry was performed to examine the cellular localization of angiogenic growth factors in control and statin-NP groups. On day 3, immunostaining for both vascular endothelial growth factor (VEGF) and fibroblast growth factor-2 (FGF-2) was observed in skeletal myocytes and blood vessels (supplemental Figure VII). On days 7 and 14, the immunostaining intensity markedly decreased in skeletal myocytes and blood vessels in the control group. In contrast, positive immunostaining was observed in endothelial cells of

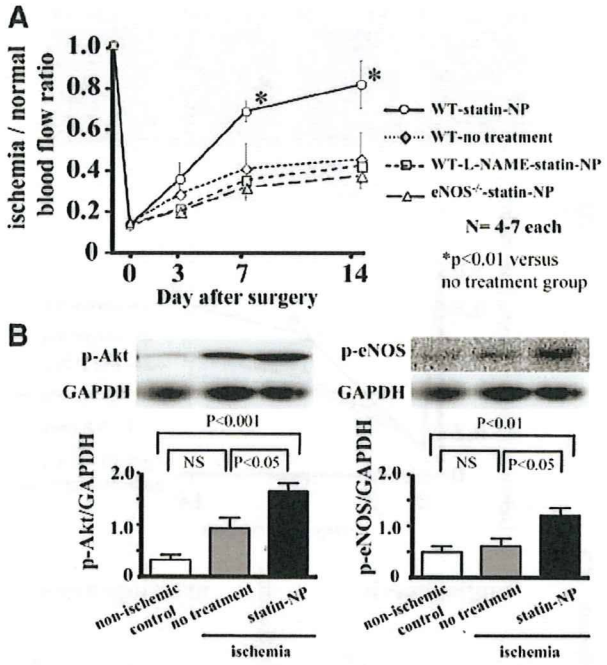

Figure 3. A, Quantification of blood flow recovery in wild-type (WT) mice with or without administration of L-NAME, a NOS inhibitor, and in $eNOS^{-/-}$ mice. B, Western blot analysis of phosphorylated Akt and eNOS in ischemic and nonischemic muscles 7 days after ischemia. n=6 each. NS=not significant.

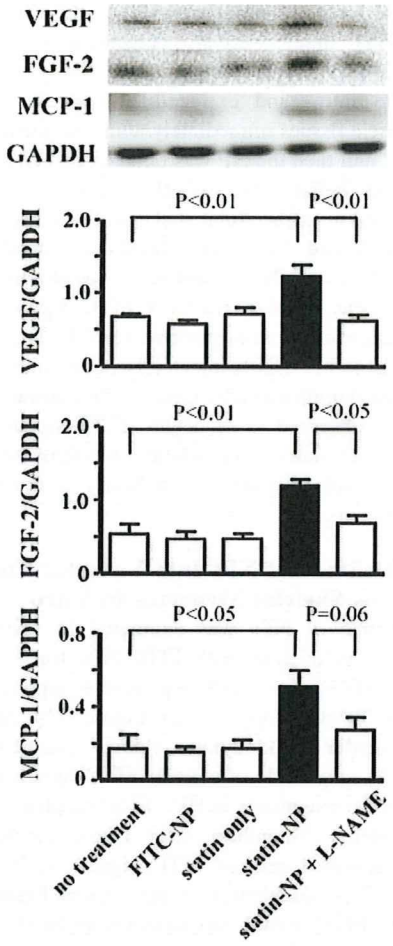

Figure 4. Effects of statin-NP on expression of VEGF, FGF-2, and MCP-1 in ischemic muscle. Densitometric analysis of protein expression in ischemic muscles 7 days after ischemia. Quantitative evaluation was expressed as a ratio of VEGF, FGF-2, and MCP-1 to GAPDH. n=6 each.

capillaries and arterioles in the statin-NP group on days 7 and 14. Western blot analysis revealed greater protein expression of VEGF, FGF-2, and monocyte chemotactic protein-1 (MCP-1) in ischemic muscle in the statin-NP group than in the no treatment group 7 days after hindlimb ischemia (Figure 4). Interestingly, the increased expression of such angiogenic growth factors by treatment with statin-NP was blunted in mice administered chronically with L-NAME.

Effects of Statin-NP on Angiogenic Capacity of Human Endothelial Cells In Vitro

Cotreatment with statin or statin-NP increased angiogenic activity in HUVECs. The angiogenic activity of statin-NP was greater than that of 10 nmol/L statin only (supplemental Figure VIIIA). Pretreatment with statin only (24-hour incubation of HUVECs with statin) had no angiogenic effects at any dose. In contrast, pretreatment with statin-NP induced significant angiogenic effects at 1 and 10 nmol/L compared with the no-treatment control group (supplemental Figure VIIIB).

Serum and Tissue Concentrations of Statin

Tissue concentrations of pitavastatin were greater in skeletal muscles injected with statin-NPs than in those injected with statin 6 and 24 hours after intramuscular administration, whereas serum levels of pitavastatin were comparable between the 2 groups (supplemental Table II). The drug was not detected in serum 1 and 3 days after injection.

Discussion

The application of nanotechnology-based drug delivery is expected to have a major impact on the development of innovative medicines. In the present study, selective NP-mediated delivery of statin to vascular endothelial cells increased neovascularization and improved tissue perfusion in a murine model of hindlimb ischemia, indicating that this novel cell-selective delivery system is feasible for therapeutic neovascularization.

The most novel finding of this study is that FITC signals were localized mainly in the vascular endothelium 7 and 14 days after injection of FITC-NP into ischemic skeletal muscles in vivo. Several factors might be involved in mechanisms of the cell-selective delivery of the NP at later time points. First, increased endocytosis of NP in the endothelium may be involved, which is based on our present experiments with CPZ, an inhibitor of clathrin-mediated endocytosis. In addition, 1-hour incubation with FITC-NP resulted in long-term and stable retention of NP in the human endothelial cells, but not in skeletal myocytes in vitro. Second, decreased exocytosis of the endothelium in the presence of ischemia might also be involved. Third, after cellular delivery of NP via endocytosis, rapid escape of the NP from the endosomal compartment to the cytoplasmic compartment may lead to

sustained intracellular drug delivery and good efficacy. The NP is likely retained in the cytoplasm where release of the encapsulated drug occurs slowly in conjunction with the hydrolysis of PLGA.[15] Overall, the nanotechnology platform for cell-selective delivery to the vascular endothelium using NP may be useful as an innovative strategy for therapeutic neovascularization and other intractable diseases.

Another important feature of this study is that a single administration of statin-NP containing pitavastatin (0.4 mg/kg) into vascular endothelial cells effectively increased therapeutic neovascularization with no serious side effect in murine model of hindlimb ischemia. Sata et al[24] reported that systemic daily administration of pitavastatin (1 mg/kg per day × 49 days=49 mg/kg) has significant therapeutic effects in mice with hindlimb ischemia. In the present study, we confirmed the study of Sata et al[24] by showing that oral daily administration of pitavastatin for 14 days (1 and 10 mg/kg per day × 14=14 and 140 mg/kg, respectively) had significant therapeutic effects, as did statin-NP (0.4 mg/kg). Therefore, our NP-mediated delivery system seems to be as effective at an approximately 100-times lower dose than the cumulative systemic dose. Furthermore, measurement of the tissue and serum concentrations of pitavastatin confirmed the effective local retention of statin-NPs in ischemic skeletal muscles in vivo. NP-mediated delivery of pitavastatin accelerated angiogenic activity of human endothelial cells in vitro. Therefore, it is possible that after NP-mediated endothelial delivery, pitavastatin was slowly released from the NPs into the cytoplasm along with PLGA hydrolysis, resulting in significant therapeutic effects.

Clearly, the therapeutic neovascularization induced by statin-NPs resulted from the pleiotropic effects, because pitavastatin-NPs had no effect on serum lipid levels. Our experiments with mice treated with a NOS inhibitor and $eNOS^{-/-}$ mice support the essential role of the eNOS pathway in the mechanism underlying the therapeutic effects of NP-mediated cell-selective delivery of statin. Consistent with the results of other investigators,[18,20,21,26] we demonstrated that pitavastatin-NP increased the activity of vascular eNOS and PI3K/Akt (as shown in supplemental Figure V) in association with an increased expression of endogenous multiple angiogenic growth factors that are involved in angiogenesis (VEGF) and arteriogenesis (FGF-2, MCP-1).[27] These therapeutic effects afforded by the NP-mediated cell-selective delivery of statin were not associated with a further increase in circulating EPC. Intramuscular injection of soluble pitavastatin alone at high doses (4 and 20 mg/kg) has no therapeutic effect, suggesting a specific advantage of endothelial cell selective delivery of pitavastatin by the PLGA NP formulation. These findings suggest that pitavastatin-NP acted locally on ischemic vascular endothelium to induce therapeutic neovascularization and are consistent with the notion that NP-mediated endothelial cell-selective delivery of statin produces a well-harmonized integrative system to form functionally mature collaterals via controlled expression of endogenous multiple angiogenic growth factors and signals, allowing for a more effective model for an integrative approach to therapeutic neovascularization.

There is a major limitation to the present study. First, we examined only a single dose of statin-NPs. It is difficult to obtain a dose-response relationship of this NP system in small animals. For translation of our present findings into clinical medicine, further studies are needed to define the dose-response relation in large animal models. This point is important because statins are reported to exert a double-edged role in angiogenesis signaling.[28] Although such antiangiogenic effects of statins at high dose did not occur in a murine model,[24] this must be examined in large animal models. Second, we only examined the therapeutic effects of a single intramuscular injection of statin-NP. Whether repetitive delivery of statin-NP at an optimal dose over time produces greater therapeutic effects remains to be investigated.

In conclusion, this platform nanotechnology of vascular endothelial cell-selective delivery of statin is a promising strategy toward more effective and integrative nanomedicine in patients with severe organ ischemia, and represents a significant advance in therapeutic neovascularization over current approaches. The nanotechnology platform may be developed further as an "integrative" approach for therapeutic neovascularization, and extended to target other molecular signals specific to vascular endothelial cells.

Acknowledgments

We thank Eiko Iwata and Miho Miyagawa for their technical supports in this study.

Sources of Funding

This study was supported by Grants-in-Aid for Scientific Research (19390216, 19650134) from the Ministry of Education, Science, and Culture, Tokyo, Japan, and by Health Science Research Grants (Research on Translational Research and Nanomedicine) from the Ministry of Health, Labor, and Welfare, Tokyo, Japan.

Disclosures

Dr Egashira holds a patent on the results reported in the present study. The remaining authors report no conflicts.

References

1. Losordo DW, Dimmeler S. Therapeutic angiogenesis and vasculogenesis for ischemic disease. Part I: angiogenic cytokines. *Circulation*. 2004;109:2487–2491.
2. Losordo DW, Dimmeler S. Therapeutic angiogenesis and vasculogenesis for ischemic disease: part II: cell-based therapies. *Circulation*. 2004;109:2692–2697.
3. Baumgartner I, Pieczek A, Manor O, Blair R, Kearney M, Walsh K, Isner JM. Constitutive expression of phVEGF165 after intramuscular gene transfer promotes collateral vessel development in patients with critical limb ischemia. *Circulation*. 1998;97:1114–1123.
4. Marui A, Tabata Y, Kojima S, Yamamoto M, Tambara K, Nishina T, Saji Y, Inui K, Hashida T, Yokoyama S, Onodera R, Ikeda T, Fukushima M, Komeda M. A novel approach to therapeutic angiogenesis for patients with critical limb ischemia by sustained release of basic fibroblast growth factor using biodegradable gelatin hydrogel: an initial report of the phase I-IIa study. *Circ J*. 2007;71:1181–1186.
5. Schaper W, Scholz D. Factors regulating arteriogenesis. *Arterioscler Thromb Vasc Biol*. 2003;23:1143–1151.
6. Heil M, Schaper W. Influence of mechanical, cellular, and molecular factors on collateral artery growth (arteriogenesis). *Circ Res*. 2004;95:449–458.
7. Ferrara N, Alitalo K. Clinical applications of angiogenic growth factors and their inhibitors. *Nat Med*. 1999;5:1359–1364.
8. Carmeliet P, Jain RK. Angiogenesis in cancer and other diseases. *Nature*. 2000;407:249–257.

9. Yonemitsu Y, Kaneda Y, Morishita R, Nakagawa K, Nakashima Y, Sueishi K. Characterization of in vivo gene transfer into the arterial wall mediated by the Sendai virus (hemagglutinating virus of Japan) liposomes: an effective tool for the in vivo study of arterial diseases. *Lab Invest*. 1996;75:313–323.
10. Ohtani K, Egashira K, Hiasa K, Zhao Q, Kitamoto S, Ishibashi M, Usui M, Inoue S, Yonemitsu Y, Sueishi K, Sata M, Shibuya M, Sunagawa K. Blockade of vascular endothelial growth factor suppresses experimental restenosis after intraluminal injury by inhibiting recruitment of monocyte lineage cells. *Circulation*. 2004;110:2444–2452.
11. Zhao Q, Egashira K, Hiasa K, Ishibashi M, Inoue S, Ohtani K, Tan C, Shibuya M, Takeshita A, Sunagawa K. Essential role of vascular endothelial growth factor and Flt-1 signals in neointimal formation after periadventitial injury. *Arterioscler Thromb Vasc Biol*. 2004;24:2284–2289.
12. Zhao Q, Egashira K, Inoue S, Usui M, Kitamoto S, Ni W, Ishibashi M, Hiasa Ki K, Ichiki T, Shibuya M, Takeshita A. Vascular endothelial growth factor is necessary in the development of arteriosclerosis by recruiting/activating monocytes in a rat model of long-term inhibition of nitric oxide synthesis. *Circulation*. 2002;105:1110–1115.
13. Celletti FL, Waugh JM, Amabile PG, Brendolan A, Hilfiker PR, Dake MD. Vascular endothelial growth factor enhances atherosclerotic plaque progression. *Nat Med*. 2001;7:425–429.
14. Kawashima Y, Yamamoto H, Takeuchi H, Hino T, Niwa T. Properties of a peptide containing DL-lactide/glycolide copolymer nanospheres prepared by novel emulsion solvent diffusion methods. *Eur J Pharm Biopharm*. 1998;45:41–48.
15. Panyam J, Zhou WZ, Prabha S, Sahoo SK, Labhasetwar V. Rapid endolysosomal escape of poly(DL-lactide-co-glycolide) nanoparticles: implications for drug and gene delivery. *Faseb J*. 2002;16:1217–1226.
16. Davda J, Labhasetwar V. Characterization of nanoparticle uptake by endothelial cells. *Int J Pharm*. 2002;233:51–59.
17. Takemoto M, Liao JK. Pleiotropic effects of 3-hydroxy-3-methylglutaryl coenzyme a reductase inhibitors. *Arterioscler Thromb Vasc Biol*. 2001; 21:1712–1719.
18. Llevadot J, Murasawa S, Kureishi Y, Uchida S, Masuda H, Kawamoto A, Walsh K, Isner JM, Asahara T. HMG-CoA reductase inhibitor mobilizes bone marrow–derived endothelial progenitor cells. *J Clin Invest*. 2001; 108:399–405.
19. Altieri DC. Statins' benefits begin to sprout. *J Clin Invest*. 2001;108: 365–366.
20. Sata M, Nishimatsu H, Suzuki E, Sugiura S, Yoshizumi M, Ouchi Y, Hirata Y, Nagai R. Endothelial nitric oxide synthase is essential for the HMG-CoA reductase inhibitor cerivastatin to promote collateral growth in response to ischemia. *Faseb J*. 2001;15:2530–2532.
21. Kureishi Y, Luo Z, Shiojima I, Bialik A, Fulton D, Lefer DJ, Sessa WC, Walsh K. The HMG-CoA reductase inhibitor simvastatin activates the protein kinase Akt and promotes angiogenesis in normocholesterolemic animals. *Nat Med*. 2000;6:1004–1010.
22. Kitamoto S, Nakano K, Hirouchi Y, Kohjimoto Y, Kitajima S, Usui M, Inoue S, Egashira K. Cholesterol-lowering independent regression and stabilization of atherosclerotic lesions by pravastatin and by antimonocyte chemoattractant protein-1 therapy in nonhuman primates. *Arterioscler Thromb Vasc Biol*. 2004;24:1522–1528.
23. Ni W, Egashira K, Kataoka C, Kitamoto S, Koyanagi M, Inoue S, Takeshita A. Antiinflammatory and antiarteriosclerotic actions of HMG-CoA reductase inhibitors in a rat model of chronic inhibition of nitric oxide synthesis. *Circ Res*. 2001;89:415–421.
24. Sata M, Nishimatsu H, Osuga J, Tanaka K, Ishizaka N, Ishibashi S, Hirata Y, Nagai R. Statins augment collateral growth in response to ischemia but they do not promote cancer and atherosclerosis. *Hypertension*. 2004;43: 1214–1220.
25. Hiasa K, Ishibashi M, Ohtani K, Inoue S, Zhao Q, Kitamoto S, Sata M, Ichiki T, Takeshita A, Egashira K. Gene transfer of stromal cell-derived factor-1alpha enhances ischemic vasculogenesis and angiogenesis via vascular endothelial growth factor/endothelial nitric oxide synthase-related pathway: next-generation chemokine therapy for therapeutic neovascularization. *Circulation*. 2004;109:2454–2461.
26. Dimmeler S, Aicher A, Vasa M, Mildner-Rihm C, Adler K, Tiemann M, Rutten H, Fichtlscherer S, Martin H, Zeiher AM. HMG-CoA reductase inhibitors (statins) increase endothelial progenitor cells via the PI 3-kinase/Akt pathway. *J Clin Invest*. 2001;108:391–397.
27. Fujii T, Yonemitsu Y, Onimaru M, Tanii M, Nakano T, Egashira K, Takehara T, Inoue M, Hasegawa M, Kuwano H, Sueishi K. Nonendothelial mesenchymal cell-derived MCP-1 is required for FGF-2-mediated therapeutic neovascularization: critical role of the inflammatory/arteriogenic pathway. *Arterioscler Thromb Vasc Biol*. 2006;26: 2483–2489.
28. Urbich C, Dernbach E, Zeiher AM, Dimmeler S. Double-edged role of statins in angiogenesis signaling. *Circ Res*. 2002;90:737–744.

Supplement Data

Therapeutic Neovascularization by Nanotechnology-Mediated Cell-Selective Delivery of Pitavastatin into the Vascular Endothelium

Mitsuki Kubo, MD; Kensuke Egashira, MD PhD; Takahiro Inoue, MD; Jun-ichiro Koga, MD; Shinichiro Oda, MD; Ling Chen, MD; Kaku Nakano, PhD; Tetsuya Matoba, MD PhD; Yoshiaki Kawashima, PhD; Kaori Hara, PhD; Hiroyuki Tsujimoto, PhD; Katsuo Sueishi, MD PhD; Ryuji Tominaga MD PhD; Kenji Sunagawa, MD PhD

Department of Cardiovascular Medicine (MK, KE, TI, JK, LC, KN, TK and K Sunagawa), Surgery (SO, RT), and Pathology (K Sueishi), Graduate School of Medical Sciences, Kyushu University, Fukuoka, Japan, School of Pharmaceutical Science (YK), Aichi Gakuin University, Aichi, Japan, and Hosokawa Powder Technology Research Institute (KH, HT), Osaka, Japan.

Supplementary Table 1.

Serum biochemical profiles 3, 7 and 14 days after hindlimb ischemia

	No treatment	FITC-NP	Statin only	Statin-NP	*P* value
Creatine Phosphokinase (IU/L)					
day 3	105±16	144±25	138±26	141±29	0.66
day 7	75±12	100±14	83±16	65±10	0.35
day 14	76±13	56±7	74±3	52±17	0.39
Myoglobin (ng/ml)					
day 3	< 10	< 10	< 10	< 10	-
day 7	< 10	< 10	< 10	< 10	-
day 14	< 10	< 10	< 10	< 10	-
AST (IU/L)					
day 3	63±10	54±24	64±14	60±16	0.97
day 7	34±1	37±6	47±8	32±7	0.37
day 14	35±7	29±2	38±5	35±3	0.57
ALT (IU/L)					
day 3	27±5	24±1	22±3	27±8	0.86
day 7	13±1	23±10	18±3	15±4	0.64
day 14	19±1	17±0	24±5	22±3	0.35
BUN (mg/dl)					
day 3	26±2.5	29±1.5	30±0.3	29±3.6	0.75
day 7	28±1	23±5	22±1	22±1	0.44
day 14	33±2	34±2	35±1	37±1	0.36
Creatinine (mg/dl)					
day 3	0.11±0.01	0.10±0.01	0.14±0.01	0.14±0.02	0.11
day 7	0.10±0.01	0.10±0.01	0.11±0.01	0.10±0.01	0.69
day 14	0.12±0.01	0.11±0.02	0.10±0.01	0.10±0.01	0.50
Total cholesterol (mg/dl)					
day 3	95±3	102±1	90±2	105±12	0.40
day 7	87±4	92±11	81±4	76±3	0.39
day 14	76±2	84±5	87±5	80±2	0.25
LDL cholesterol (mg/dl)					
day 3	24±2	22±2	24±3	27±5	0.72
day 7	12±2	21±9	15±2	13±2	0.56
day 14	5±1	5±0	8±1	7±2	0.33

Data are mean±SEM (n=3 each)

Supplementary Table 2.

Tissue and serum pitavastatin concentrations after intramuscular injection of statin

	time after injection		
	6 hours	1 day	3 day
Pitavastatin at 0.4 mg/kg			
muscle (ng/g tissue)	305 ± 80	81 ± 60	4 ± 3
serum (ng/ml)	3 ± 0.3	ND	ND
Statin-NP containing 0.4 mg/kg of pitavastatin			
muscle (ng/g tissue)	2088 ± 412*	692 ± 288*	9 ± 5
serum (ng/ml)	5 ± 0.7	ND	ND

Data are mean±SEM (n=8 to 9 each). ND: not detected. *P<0.01 versus intramuscular pitavastatin.

Supplementary Figure Legends

Supplementary Figure I. Immunofluorescent staining of cross-sections from ischemic muscle 14 days after FITC-NP injection stained with an endothelial marker, CD31 (red). Inset left below is non-injected control muscle. Scale bars: 100 μm.

Supplementary Figure II. Cell-selective delivery of FITC-NP into vascular endothelial cells versus skeletal myocytes. A, Fluorescent micrographs of HUVEC and SkMC incubated with FITC-NP (0.1 mg/ml) for 1 hour and percentage of FITC-positive cells (n=5 each). Nuclei were counter stained with PI. Scale bars: 100 μm. B, Effects of chlorpromazine (CPZ) on cellular distribution of NP in HUVEC and SkMC. Quantitative analysis of magnitude of intracellular FITC fluorescence signals in 3 independent experiments are shown. *$p<0.05$, **$p<0.001$ versus control condition. C, Fluorescent micrographs of HUVEC immediately after, and 3 and 7 days after the 1 hour incubation with FITC-NPs. Inset left above is control HUVEC without FITC-NP. Nuclei were counter stained with PI. Scale bars: 100 μm.

Supplementary Figure III. A, Quantification of LDPI–derived blood flow recovery expressed as the ratio of ischemic to normal limb at 7 and 14 days. Mice were injected with pitavastatin at 4 and 20 mg/kg into the ischemic muscle immediately after induction of hindlimb ischemia. N = 5 to 6. NS=no significance. B, Representative scatter diagram of Sca-1/Flk-1-double positive EPCs in peripheral blood analyzed by flow cytometry 14 days after induction of hindlimb ischemia (circled region). C, Quantitative analysis of circulating EPCs expressed as percentage of Sca-1/Flk-1 double positive cells to total leukocytes 7 and 14 days after ischemia. N = 4 to 5 each. *$p<0.05$, **$p<0.001$ versus non-ischemic control group.

Supplementary Figure IV. Effects of oral daily administration of pitavastatin on ischemia-induced neovascularization. Quantification of laser Doppler perfusion imaging (LDPI)–derived blood flow recovery at 14 days. n=6 to 8. *$p<0.05$, **$p<0.01$ versus no treatment group.

Supplementary Figure V. Schematic illustration of the effects of statins on intracellular pathways. Mevalonate, the end product of the HMG-CoA, inhibits PI3K and the subsequent phosphorylation of Akt and eNOS. Blockade of HMG-CoA reductase with statins is expected to result in the increase of activity of Akt and eNOS.

Supplementary Figure VI. Representative micrographs of ischemic muscle sections stained immunohistochemically with antibodies against phospho-Akt and phospho-eNOS at 14 days after surgery. Scale bars: 100 μm.

Supplementary Figure VII. Effects of statin-NP on the protein expression of VEGF (A) and FGF-2 (B) in ischemic muscle. Representative photographs of immunostaing of ischemic muscles 3, 7, and 14 days after hindlimb ischemia. VEGF or FGF-2 (green) is located not only within myocytes but within capillary or vascular endothelium (yellow) on day 7 and 14 in statin-NP group. Nuclei were counter stained with DAPI (blue). Scale bars: 100 μm.

Supplementary Figure VIII. Effects of statin-NP on angiogenic capacity of human endothelial cells in vitro. A, Quantitative analysis of tube formation (tube length) of 4

independent experiments in co-treatment protocol. *$p<0.01$, **$p<0.001$ vs control. B, Quantitative analysis of tube formation (tube length) of 4 independent experiments in pre-treatment protocol. *$p<0.05$, **$p<0.001$ versus control.